RSC Advances

PAPER

View Article Online
View Journal | View Issue

Cite this: *RSC Adv.*, 2020, **10**, 21650

Alkynyl- and phosphine-ligated quaternary Au_2Ag_2 clusters featuring an Alkynyl-AuAg motif for multicomponent coupling

Quanquan Shi,[a] Zhaoxian Qin,[c] Guichen Ping,*[a] Shuang Liu,[bc] Hui Xu[a] and Gao Li *[c]

The coordination motif of alkynly with a metal atom is versatile and plays a pivotal role in tailoring the kernel configuration of the atomically precise metal nanoclusters. In this study, we synthesized a new mono-valent $Au(I)_2Ag(I)_2(C_{10}H_6NO)_4(Ph_3P)_2$ alloy cluster with a very high yield of >90%, which is well characterized by a serial of technologies, *e.g.* UV-vis, X-ray single crystal diffraction (SCXRD) and FT-IR. The SCXRD analysis shows the alloy cluster is composed of a quadrangular Au_2Ag_2 kernel protected by four alkynyl and two phosphine ligands. Intriguingly, a new divergent alkyne-metal coordination model is revealed in this cluster, the alkynyl ligands selectively bind to Au and Ag atoms *via* σ- and π-bond configurations and adopt a VI-shaped alkynyl-M motif. It is distinct from the convergent motif observed in big clusters featuring an IV- or V-shaped alkynyl-M motif due to the steric effect. Finally, the titanium oxide-supported Au_2Ag_2 cluster catalysts show good catalytic performance in the multicomponent coupling reaction of alkynes, aldehydes and amines.

Received 8th March 2020
Accepted 1st June 2020

DOI: 10.1039/d0ra02178d

rsc.li/rsc-advances

Introduction

Metal nanoclusters protected by monolayer organic ligands have drawn increasing interest for their unique structures and properties which differ from those of metal atoms and bulk metal.[1–5] Recently, it has been reported that nanoclusters show great potential application in fundamental studies: photoluminescence, bio-imaging, medicine and catalysis.[6–9] But revealing their structure is not always possible in this field. With the developments in nanotechnology, some big molecule-like metal nanoclusters having different core structures and sizes have been determined by X-ray single crystal diffraction.[10–14] For the application of newly discovered materials, there is no doubt that the insight into their nanostructure at the atomic level is helpful for the understanding of the relationship between structures and properties, which is an indispensable step for exploring the application of these nanomaterials.

Generally, the shapes, sizes and properties of metal nanoclusters will be affected deeply by the protecting ligands on the outmost surface, which not only enhances the stability against aggregation, but generates significant interfaces related to optical, catalytic, biological and sensing applications.[15–19] To data, five types of ligands have been used as protecting ligands for the atomically precise metal nanoclusters, including thiolate, phosphine, halogen, alkynyl and carbene; the former three ligands are extensively studied for many years, and alkynyl and carbene ligands are used as an emerging ligands.[20–24] Due to their special and different coordination models, the co-present of two or three of them is more efficient for the stability of nanoclusters. In details, thiolate may take a μ_2-η^1-η^1 model coordinate with two metal atoms on the surface of core forming staple motifs.[15] Carbene and phosphine take a μ_1 coordination model *via* σ bonds.[25,26] A halide could coordinate with four metal atoms at most. The situation of alkynyl is very complex for the presence of π electrons which will be the focus of present work. What's more, in the alkynyl protected nanoclusters, the metal species in core will affect the coordination model in return.[15] There are some possible coordination motifs in theory shown in Scheme 1. Far as we know, I- to V-shape occurred in homogeneous and heterogeneous clusters have been reported by Tsukuda and Wang successively.[27,28] The VI-shape different from the five convergent motifs is a divergent motif which is not good for the formation of zero-dimension structures. Therefore, whether it is possible for the existence of motif VI in clusters still remained unknown yet.

Herein, we report a quaternary clusters $Au^I_2Ag^I_2(L)_4(PPh_3)_2$ (where L represents 2-(prop-2-ynyloxy)benzonitrile, short as Au_2Ag_2, hereafter) ligated by alkynelate and phosphine ligands. The structure of the alloy cluster was revealed by X-ray single crystal diffraction analysis. The small Au_2Ag_2 clusters adopt a VI alkynelate motif, and it is constructed by two parallel L–($AgPPh_3$)–Au–($AgPPh_3$)–L motif by sharing the silver atoms. The Au_2Ag_2 cluster, supported onto TiO_2, shows good catalytic performance in

[a]*College of Science & Inner Mongolia Key Laboratory of Soil Quality and Nutrient Resource, Inner Mongolia Agricultural University, Hohhot 010018, China*

[b]*School of Chemistry and Chemical Engineering, Qufu Normal University, Qufu 273165, China*

[c]*State Key Laboratory of Catalysis, Dalian Institute of Chemical Physics, Chinese Academy of Sciences, Dalian 116023, China. E-mail: gaoli@dicp.ac.cn*

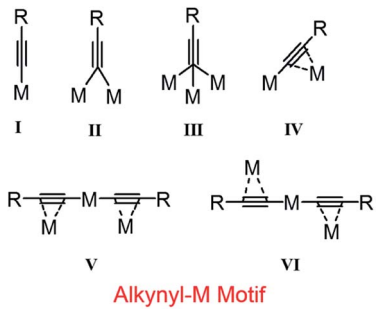

Scheme 1 The alkynyl-metal (M: Au and Ag) interfacial bonding models in theory.

the multicomponent coupling reaction of alkynes, aldehydes and amines.

Experimental

Chemicals and method

All chemicals, including solvents, were commercially available as reagent grade and used as received without further purification. Me_2SAuCl (98%), $AgBF_4$ (99%), $NaBH_4$ (99%) 2-hydroxybenzonitrile and 3-bromoprop-1-yne were purchased from Adamas-beta®. 2-(Prop-2-ynyloxy)benzonitrile was synthesized in our lab according to reported method.[29] Ultrapure water was purified with a Barnstead Nanopure Di-water TM system. All glassware was thoroughly cleaned with aqua regia (37 wt% HCl : HNO_3 = 3 : 1 by volume), rinsed with copious Nano-pure water, and then dried in an oven prior to use. UV-vis spectra of the clusters were acquired on a Hewlett-Packard (HP) Agilent 8453 diode array spectrophotometer. A sample of 2 mg was dissolved into dissolved in a 4 mL CH_2Cl_2/methanol solution and prepared for test at room temperature. FT-IR measurements were recorded on a Thermo/ATI/Mattson 60AR instrument (resolution: 1 cm^{-1}, scans: 16, range: 600–4000 cm^{-1}). The samples were prepared by spotting a CH_2Cl_2/methanol solution of the clusters onto a NaCl window.

Synthesis of 2-(prop-2-ynyloxy)benzonitrile (abbreviated as H–L, hereafter) ligand

2-Hydroxybenzonitrile of 10 mmol was refluxed with 15 mmol K_2CO_3 and 12.5 mmol 3-bromoprop-1-yne in an acetone solution for 24 hours at 80 °C. Upon completion, the solid was removed by filtration, and the filtrate was dried by rotate evaporation. The crude product was further purified by silica gel using only dichloromethane as eluent. ^1H NMR (600 MH_Z, $CDCl_3$): δ 7.55–7.60 (m, 2H), 7.05–7.26 (m, 2H), 4.84 (s, 2H), 2.57 (s, 1H). IR (cm^{-1}): ν 3286 (*vs.*, C≡C–H), 2223 (*vs.*, C≡N), 2120 (vw, C≡C).

Synthesis of Au/Ag–L complex

HL of 186 mg was dissolved with NEt_3 (1 eq.) into dichloromethane of 20 mL, followed by the addition of a solution of dichloromethane containing 294 mg Me_2SAuCl dropwise under stirring. The mixture was kept stirring in dark in air for an hour, forming a clear solution. Then the solvent was removed by rotate evaporation, giving a dark green mixture. The light blue neat product was obtained by washing with methanol and diethyl ether. The slight blue solid should be stored in dark and cool place. The L–Ag complex was prepared using the similar method, expect the Me_2SAuCl was replaced by $AgBF_4$.

Synthesis of $Au_2Ag_2(L)_4(Ph_3P)_2$ clusters

The synthesis method of the Au_2Ag_2 clusters was designed according to a bottom-up strategy. L–Au of 20 mg and L–Ag of 20 mg were mixed in a mixture solution of 4 mL dichloromethane and methanol (v/v = 1 : 1) under rapid stirring for ~30 min, giving a yellow suspension. Ph_3P of 10 mg was then added slowly. Notably, the addition of phosphine ligands can largely improve the solubility of the alkynyl-Ag/Au complexes *via* a reaction (alkynyl-Ag/Au + PPh_3 → alkynyl-Ag/Au–PPh_3) in the dichloromethane and methanol solutions, and the capped phosphine ligands on surface of metal clusters can facilitate crystallization. After ~24 h, a brown mixture was obtained. The solid was then removed by filtration, and the filtrate was diffused by ether in dark. A high yield of over 90%, based on the consumption of Me_2SAuCl, is achieved. After two weeks, the yellow block crystals of Au_2Ag_2 cluster was obtained. IR (cm^{-1}): 2230 (*vs.*, C≡N), 2122 (vw, C≡C). 1646 (s, H–Ar).

X-ray crystallographic analysis

Data reduction, cell refinement and experimental absorption correction were performed with the software package of CrysAlis^{pro}. The structures were solved by intrinsic phasing methods by ShelXT 2018 and refined against F^2 by full-matrix least-squares by ShelXL 2018.[30,31] All non-hydrogen atoms were refined anisotropically. Hydrogen atoms were generated geometrically. All calculations were carried out by the program package of program package ver 1.2.10.[32]

Crystal data and structure refinements

Crystal data for $[Ag_2Au_2(L)_4(Ph_3P)_2]$, triclinic, $P\bar{1}$ (no. 2), a = 14.4910(2) Å, b = 17.5030(2) Å, c = 29.1650(4) Å, α = 99.2440(10)°, β = 101.1180(10)°, γ = 107.5380(10)°, V = 6729.25(16) $Å^3$, Z = 1, T = 273.15 K, 78 562 reflections measured, R_1 = 0.0688, wR_2 = 0.1724. CCDC-1972447 contain the supplementary crystallographic data in this paper.

Preparation of TiO_2-supported metal clusters

Typically, 5 mg metal cluster $(Ag_2Au_2(L)_4(Ph_3P)_2$, $Au_{25}(PPh_3)_{10}(C_2Ph)_5X_2$ and $Au_{13}(Ph_2C_3H_6Ph_2)Cl_2)$ was dissolved in 50 mL methanol, and 1 g TiO_2 powder was added. After stirred for ~3 h at room temperature, the supernatant became colorless. These Au_2Ag_2/oxide catalysts were collected by centrifugation and dried under vacuum. Then these oxide-supported Au_2Ag_2 catalysts of *ca.* 1 wt% cluster loading were annealed at 100 °C in a vacuum oven for 1 h prior to the catalytic evaluations.

Typical procedure for the multicomponent coupling reaction

In a typical three-component coupling reaction, benzaldehyde (1 mmol), phenylacetylene (1.3 mmol), piperidine (1.2 mmol),

metal clusters/oxide (100 mg), and 5 mL water were added to a 10 mL vial. The mixture was stirred under N_2 atmosphere at 80 °C for 16 h as indicated in Table 2. The catalysts were separated and collected by centrifugation, washed with water and EtOAc to remove salts and organic compounds, respectively, and dried under vacuum. The products were identified by ^{1}H NMR using the $CDCl_3$ as solvent.

Results and discussion

Synthesis of Au_2Ag_2 clusters

The alkynyl protected Au^IAg^I alloy nanoclusters were prepared by the simply self-assembly of alkynyl-Au^I and alkynyl-Ag^I complexes in the presence of phosphine in a dichloromethane and methanol solution. The prepared clusters only gave one optical peak at 326 nm (Fig. 1), which might be caused by the ligand–metal charge transformation (LMCT)[33,34] assigned to the adsorption of the M–PPh_3 groups (where, M = Au or Ag). Further, the structures of Au_2Ag_2 cluster are determined by X-ray single-crystal diffraction, as shown in Fig. 2a. This small alloy cluster is crystallized in a triclinic system with a $P\bar{1}$ group. SCXRD suggests that this cluster is composed by 2 Au atoms, 2 Ag atoms, 2 Ph_3P ligands and 4 L ligands. Intriguingly, the L ligands are coordinated with gold and silver atoms in an IV type (Scheme 1), and the phosphine ligands only bind with the silver atoms. It worthy to note that the preparation of the homologous $Au^I_4(L)_4(PPh_3)_2$ and $Ag^I_4(L)_4(PPh_3)_2$ clusters were unsuccessful using the same protocol.

Crystal structure of Au_2Ag_2 clusters

The screening of the Au_2Ag_2 clusters is depicted in the Table 1. Interestingly, the two gold atoms and two silver atoms are located in a plane to give a parallelogram. In details, the two Au atoms interact with another two Ag atoms in the same plane *via* strong the Au–Ag bonds (length of 2.957(2) Å to 3.112(4) Å), forming a parallelogram where the Au and Ag atoms are arranged right on the diagonal, respectively (Fig. 2b). Of note, the distance of two Au atoms is 3.648 Å, which is much longer than the Au–Au bond (*e.g.* <2.8 Å).[4,13] The angles constructed by the Au–Ag–Au and Ag–Au–Ag in the parallelogram are 73.876(1)° and 106.125(1)°, respectively.

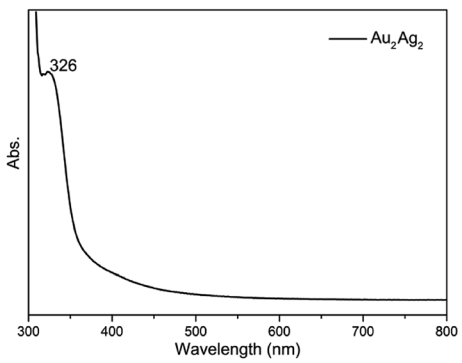

Fig. 1 UV-vis spectrum of the prepared $Au_2Ag_2(L)_4(Ph_3P)_2$ clusters (dissolved in a CH_2Cl_2/methanol solution).

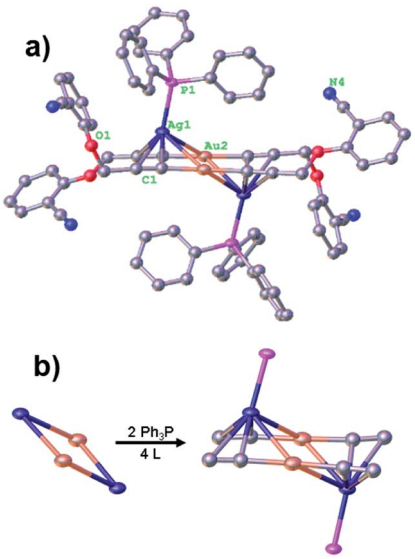

Fig. 2 (a) The full structure of $Au_2Ag_2(L)_4(Ph_3P)_2$ with 30% probably ellipsoids. (b) The core structure and coordination model in Au_2Ag_2 clusters. Color code: Au, gold; Ag, dark blue; P, pink; O, red; N, blue; C, grey. H atoms are omitted for clarity.

The four-member core was protected by four L ligands *via* σ-bonds and π-bonds (more details are listed in Table 1). A pair of L ligands from different side of the place constructed by Au_2Ag_2 core coordinated with same Au atom *via* σ-bond (1.992(8) Å in average) to give an L–Au–L unit. Two L–Au–L units further linked by two Ag atoms in parallel forming a new plane *via* π-bonds which is ~2.624(6) Å, furnishing a dihedral angle of 35.547(9) ° with Au_2Ag_2 core plane. Of note, the Ag atoms interact with L ligands *via* σ-bond give rise to two sides (VI-mode in Scheme 1), rather than one side (V-mode). This is different from the reported big metal clusters, which is caused by the steric effects of the bulky ligands (*e.g.* P*Ph*$_3$, –C≡C–*Ar*) on the surface of the metal clusters.[15] In short, the alkynyl ligands selectively bind to Au and Ag atoms through σ- and π-bond, respectively, which may be the reason why the homologous $Au^I_4(L)_4(PPh_3)_2$ and $Ag^I_4(L)_4(PPh_3)_2$ clusters cannot be prepared under the similar synthetic conditions. Thus, most part of Ag

Table 1 List of the average bond lengths and angles in the Au_2Ag_2 clusters. Where, C_T represents the terminal carbon of the ligated alkyne ligands

Entry	Lengths and angle	Average	Scope
1	Au–Au	3.648 Å	—
2	Au–Ag	3.006 Å	2.957–3.112 Å
3	Au–C_T	1.984 Å	1.942–2.023 Å
4	Ag–C_T	2.386 Å	2.337–2.438 Å
5	Ag–P	2.418 Å	2.426 & 2.410 Å
6	Au–Ag–Au	73.876°	—
7	Ag–Au–Ag	106.125°	—

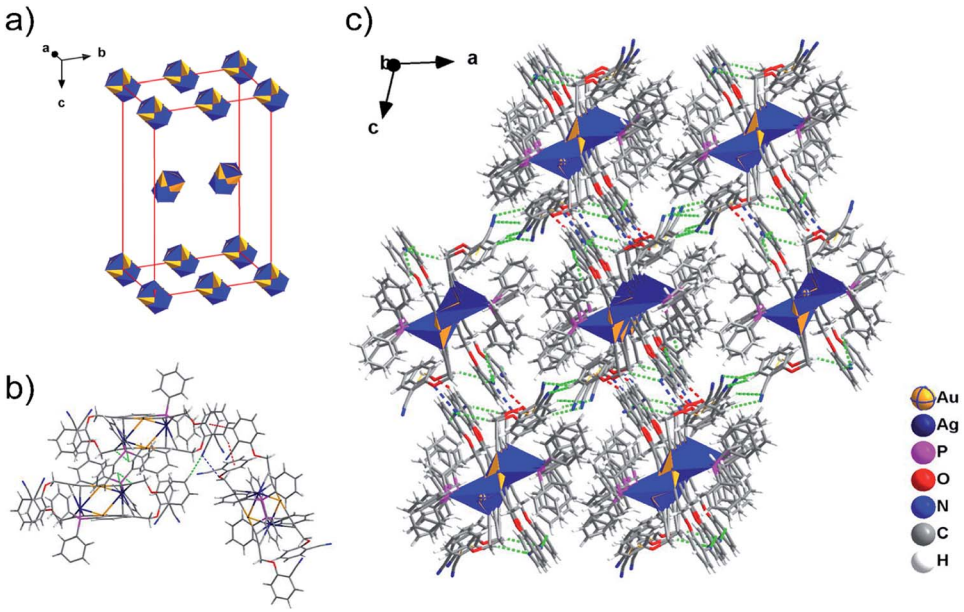

Fig. 3 (a) Au_2Ag_2 clusters in one cell unit. (b) The intermolecular interactions between Au_2Ag_2 clusters. (c) The packing model of Au_2Ag_2 cluster along *b*-direction. The uncoordinated atoms in (a) are omitted for clarity.

atoms are bare, which is a good chance for the coordination of Ph_3P. And the PPh_3 ligand is very smart to catch this chance. Two Ph_3P ligands coordinate through P–Ag bonds (2.418(9) Å) with the half-bare Ag atoms taking a typical top model. The presence of Ph_3P is very important for the formation of this cluster to restrict its size in space.

In each cell of crystal, there are about 4 ($2 \times 1 + 8 \times 1/8 + 4 \times 1/4$) clusters contained, two in the centre of the cell ($2 \times 1 = 2$ clusters), eight on the vertexes ($8 \times 1/8 = 1$ cluster) and four at the centre of edges ($4 \times 1/4 = 1$ cluster), respectively, as shown in Fig. 3a. The two clusters in the centre of cell interact with each other through intermolecular force including C···C (~3.3 Å) van der Waals' force, $N\cdots H_{phenyl}$ hydrogen bonds (~2.738 Å) and unique $H\cdots\pi_{alkynyl}$ (~2.822 Å) interactions for which the special arrangement of L ligands in clusters should be responsible (Fig. 3b). The two clusters in cell further interact with outside cluster molecular through N···O (~3.0 Å) van der Waals' force and $H\cdots\pi_{phenyl}$ (2.60 Å in average) interactions form the three-dimensional framework (Fig. 3c).

We further suited the IR spectra of Au_2Ag_2 cluster, which was then compared with IR of HL, as depicted in Fig. 4, compared with HL, the most representative peaks near 3286 cm^{-1} assigned to strong H–C≡C stretching vibration almost disappeared in the FT-IR spectra of Au_2Ag_2 clusters, indicating that the H atoms linked to the terminal carbon of H–L was removed and bonded by metal atoms. Besides, the peak in the scale of 2220–2230 cm^{-1} assigned to the vibration of C≡N bonds remained unchanged basically, indicating that the C≡N group in L did not take part in the coordination with metal atoms, which is in good line with the SCXRD results as well. The strong peak near 1646 cm^{-1} should be assigned to the presence of Ph_3P ligands in Au_2Ag_2. The two peaks near 2842 and 2922 cm^{-1} should be caused by the strong stretching vibration of C–H bonds from CH_2 group. In all, these FT-IR results highly match with the $Au_2Ag_2(L)_4(Ph_3P)_2$ structure convinced by SCXRD.

In recent decade, the metal clusters have been utilized to be a novel and promising catalyst in the carbon–carbon coupling reaction, which generate new chemicals, such as alkaloids as well as in numerous biologically active parts of pharmaceutical and agrochemical specialities.[35–38] The Au_2Ag_2 nanoclusters, capped by alkyne ligand, can be a good catalyst to incur the activation of alkynes, which is the key step during the multicomponent-coupling reactions of benzaldehyde, piperidine and phenylacetylene. In our previous studies, we have found that the alkyne/phosphine capped $Au_{25}(PPh_3)_{10}(C_2Ph)_5X_2$ clusters have showed promising catalytic performance in the multicomponent-coupling reactions.[39] Therefore, we decided to investigate the catalytic performance of Au_2Ag_2 clusters in the multicomponent coupling reactions to yield the product of

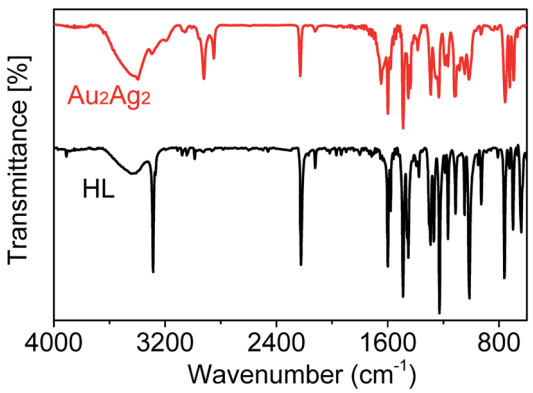

Fig. 4 Comparison of the IR spectra of prepared Au_2Ag_2 clusters (red line) and free HL ligands (black line).

Table 2 Screening of the catalytic performance of clusters as the catalysts for multicomponent coupling reaction of benzaldehyde, piperidine and phenylacetylene[a]

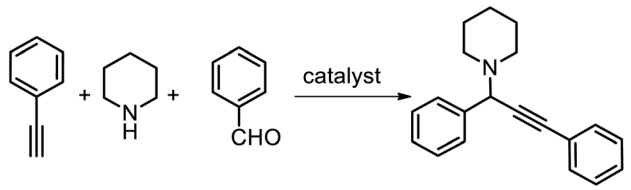

Entry	Catalyst	Yield[b]
1	TiO_2	n.d.
2	Au_2Ag_2/TiO_2	81%
3	Au_{25}/TiO_2	62%
4	Au_{13}/TiO_2	45%
5[c]	Au_2Ag_2/TiO_2	80%
6[d]	Au_2Ag_2/TiO_2	79%

[a] Reaction conditions: 100 mg metal clusters/TiO_2 catalysts, 1.0 mmol benzaldehyde, 1.2 mmol piperidine, 1.3 mmol phenylacetylene, 5 mL water, 16 h, under a N_2 atmosphere; n.d. = not detected. [b] The yield of propargylamine was determined by ^1H NMR. [c] 2nd reuse of the catalyst recovered from entry 2. [d] 3rd reuse of the catalyst recovered from entry 5.

propargylamine in this work. These clusters were immobilized on the TiO_2 *via* an impregnation method of the oxide powders in a methanolic solution of the clusters. These test results are compiled in Table 2. Surprisingly, the Au_2Ag_2/TiO_2 catalysts gave rise to a promising activity; an 81% yield of propargylamine was achieved, Table 2, entry 2. For comparison, the alkynyl- and phosphine-ligated $Au_{25}(PPh_3)_{10}(C_2Ph)_5X_2$ (shorten as Au_{25}) and phosphine-protected $Au_{13}(Ph_2C_3H_6Ph_2)Cl_2$ (shorten as Au_{13}) were synthesized for the coupling reactions.[39,40] The large-sized Au_{25} showed some lower activity; a 62% yield was obtained (Table 2, entry 3). And a much low yield of 45% was found when the multicomponent coupling reaction was catalyzed over the Au_{13}/TiO_2 catalysts (Table 2, entry 4). The prominent activity of the alloy clusters is mainly due to the steric effect; the small-sized particles can provide more catalytically active sites during the multicomponent coupling reactions. It is worthy to note that the plain TiO_2 supports were inactivity during the multicomponent coupling reaction, which implies that the catalytic reactions should be occurred over the metal clusters.

Further we examined the catalytic activity of the reused Au_2Ag_2/TiO_2 to evaluate the recyclability of the alloy clusters. A fresh reaction was carried out using the recycled catalyst with reactants in fresh water under the identical reaction conditions. It is found that recycled catalyst yields nearly the same activity as fresh catalyst (Table 2, entries 5 and 6). After three cycles, no appreciable loss of catalytic activity was observed; thus, Au_2Ag_2/TiO_2 is deemed as a good recyclable catalyst for the multicomponent coupling reactions.

Conclusions

In summary, a new mono-valence $Au_2Ag_2(C_{10}H_6NO)_4(Ph_3P)_2$ alloy cluster is prepared. Its nanostructure is well studied by SCXRD analysis, showing that this cluster is composed of an Au_2Ag_2 core protected by alkynyl and phosphine ligands forming a bimetal quaternary cluster. Notably, a new divergent alkyne-metal coordination model is revealed, which is different to the convergent motif found in big clusters. Besides, the selectivity of alkynyl show up in this case, which coordinate with Ag and Au *via* π bonds and σ binds respectively. The structural revealing of small clusters makes it possible for the further understanding of growth process from the small to big ones. The Au_2Ag_2 alloy clusters exhibit good catalytic performance in the carbon–carbon coupling reactions.

Conflicts of interest

There are no conflicts to declare.

Acknowledgements

Q. S. acknowledges financial support by the National Natural Science Foundation of China (21665020), the Postdoctoral Science Foundation of China (223232), the Natural Science Foundation of Inner Mongolia Autonomous Region (2018BS02004, 2017MS0203), the Young Talents of Science and Technology in Universities of Inner Mongolia Autonomous Region (NJYT-20-B20), the Program of Higher-level Talents of Inner Mongolia Agricultural University (NDYB2016-03).

Notes and references

1 R. C. Jin, *Nanoscale*, 2015, **7**, 1549–1565.
2 M. Zhou, C. J. Zeng, Y. X. Chen, S. Zhao, M. Y. Sfeir, M. Z. Zhu and R. C. Jin, *Nat. Commun.*, 2016, **7**, 7.
3 R. R. Nasaruddin, T. K. Chen, N. Yan and J. P. Xie, *Coord. Chem. Rev.*, 2018, **368**, 60–79.
4 Z. Qin, D. Zhao, L. Zhao, Q. Xiao, T. Wu, J. Zhang, C. Q. Wan and G. Li, *Nanoscale Adv.*, 2019, **1**, 2529–2536.
5 S. Theivendran, L. Chang, A. Mukherjee, L. Sementa, M. Stener, A. Fortunelli and A. Dass, *J. Phys. Chem. C*, 2018, **122**, 4524–4531.
6 S. Maity, D. Bain and A. Patra, *Nanoscale*, 2019, **11**, 22685–22723.
7 G. Li and R. C. Jin, *Acc. Chem. Res.*, 2013, **46**, 1749–1758.
8 H. Chen, Z. Li, Z. Qin, H. Kim, H. Abroshan and G. Li, *ACS Appl. Nano Mater.*, 2019, **2**, 2999–3006.
9 S. Guo, Q. Fang, Z. Li, J. Zhang and G. Li, *Nanoscale*, 2019, **11**, 1326–1334.
10 Z. Lei, X. K. Wan, S. F. Yuan, Z. J. Guan and Q. M. Wang, *Acc. Chem. Res.*, 2018, **51**, 2465–2474.
11 Y. Negishi, S. Hashimoto, A. Ebina, K. Hamada, K. Wakamatsu and Y. Niihori, *Bunseki Kagaku*, 2019, **68**, 825–838.
12 G. Li, H. Abroshan, C. Liu, S. Zhuo, Z. Li, Y. Xie, H. J. Kim, N. L. Rosi and R. Jin, *ACS Nano*, 2016, **10**, 7998–8005.

13 C. Zhang, Y. Chen, H. Wang, Z. Li, K. Zheng, S. Li and G. Li, *Nano Res.*, 2018, **11**, 2139–2148.
14 Z. Lei, J. J. Li, X. K. Wan, W. H. Zhang and Q. M. Wang, *Angew. Chem., Int. Ed.*, 2018, **57**, 8639–8643.
15 Y. Wang, X. K. Wan, H. Ren, F. Su, G. Li, S. Malola, S. C. Lin, Z. C. Tang, H. Hakkinen, B. K. Teo, Q. M. Wang and N. F. Zheng, *J. Am. Chem. Soc.*, 2016, **138**, 3278–3281.
16 Z. Li, C. Liu, H. Abroshan, D. R. Kauffman and G. Li, *ACS Catal.*, 2017, **7**, 3368–3374.
17 C. Yan, C. Liu, H. Abroshan, Z. Li, R. Qiu and G. Li, *Phys. Chem. Chem. Phys.*, 2016, **18**, 23358–23364.
18 A. Mathew, G. Natarajan, L. Lehtovaara, H. Hakkinen, R. M. Kumar, V. Subramanian, A. Jaleel and T. Pradeep, *ACS Nano*, 2014, **8**, 139–152.
19 S. Antonello, G. Arrigoni, T. Dainese, M. D. Nardi, G. Parisio, L. Perotti, A. Rene, A. Venzo and F. Maran, *ACS Nano*, 2014, **8**, 2788–2795.
20 Z. Lei and Q. M. Wang, *Coord. Chem. Rev.*, 2019, **378**, 382–394.
21 P. Maity, S. Takano, S. Yamazoe, T. Wakabayashi and T. Tsukuda, *J. Am. Chem. Soc.*, 2013, **135**, 9450–9457.
22 M. R. Narouz, S. Takano, P. A. Lummis, T. I. Levchenko, A. Nazemi, S. Kaappa, S. Malola, G. Yousefalizadeh, L. A. Calhoun, K. G. Stamplecoskie, H. Hakkinen, T. Tsukuda and C. M. Crudden, *J. Am. Chem. Soc.*, 2019, **141**, 14997–15002.
23 C. Liu, T. Li, H. Abroshan, Z. Li, C. Zhang, H. J. Kim, G. Li and R. Jin, *Nat. Commun.*, 2018, **9**, 744.
24 K. Zheng, J. Zhang, D. Zhao, Y. Yang, Z. Li and G. Li, *Nano Res.*, 2019, **12**, 501–507.
25 H. Shen, G. C. Deng, S. Kaappa, T. D. Tan, Y. Z. Han, S. Malola, S. C. Lin, B. K. Teo, H. Hakkinen and N. F. Zheng, *Angew. Chem., Int. Ed.*, 2019, **58**, 17731–17735.
26 A. Munoz-Castro, *Inorg. Chem. Front.*, 2019, **6**, 2349–2358.
27 S. Ito, S. Takano and T. Tsukuda, *J. Phys. Chem. Lett.*, 2019, **10**, 6892–6896.
28 X. K. Wan, Q. Tang, S. F. Yuan, D. E. Jiang and Q. M. Wang, *J. Am. Chem. Soc.*, 2015, **137**, 652–655.
29 J. Li, F. Yang, Y. T. Ma and K. Ji, *Adv. Synth. Catal.*, 2019, **361**, 2148–2153.
30 O. V. Dolomanov, L. J. Bourhis, R. J. Gildea, J. A. K. Howard and H. Puschmann, *J. Appl. Crystallogr.*, 2009, **42**, 339–341.
31 G. M. Sheldrick, *Acta Crystallogr., Sect. A: Cryst. Phys., Diffr., Theor. Gen. Crystallogr.*, 2015, **71**, 3–8.
32 G. M. Sheldrick, *Acta Crystallogr., Sect. C: Cryst. Struct. Commun.*, 2015, **71**, 3–8.
33 H. R. C. Jaw and W. R. Mason, *Inorg. Chem.*, 1989, **28**, 4370–4373.
34 R. Arayanaswamy, M. A. Young, E. Parkhurst, M. Ouellette, M. E. Kerr, D. M. Ho, R. C. Elder, A. E. Bruce and M. R. M. Bruce, *Inorg. Chem.*, 1993, **32**, 2506–2517.
35 G. Li and R. Jin, *Nanotechnol. Rev.*, 2013, **5**, 529–545.
36 Y. Zhou and G. Li, *Acta Phys. Sin.*, 2017, **33**, 1297–1309.
37 Z. Li, X. Yang, C. Liu, J. Wang and G. Li, *Prog. Nat. Sci.: Mater. Int.*, 2016, **26**, 477–482.
38 J. Lin, H. Abroshan, C. Liu, M. Zhu, G. Li and M. Haruta, *J. Catal.*, 2015, **330**, 354–361.
39 Y. Chen, C. Liu, H. Abroshan, J. Wang, Z. Li, G. Li and M. Haruta, *J. Catal.*, 2016, **337**, 287–294.
40 J. Zhang, Y. Zhou, K. Zheng, H. Abroshan, D. R. Kauffman, J. Sun and G. Li, *Nano Res.*, 2018, **11**, 5787–5798.